Journal Pre-proof

Axial-symmetric conjugated group promoting intramolecular charge transfer performances of triphenylamine sensitizers for dye-sensitized solar cells

Shaorui Chen, Juan Pei, Zhihan Pang, Wenjun Wu, Xudong Yu, Cong Zhang
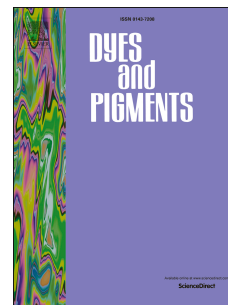
Please cite this article as: Chen S, Pei J, Pang Z, Wu W, Yu X, Zhang C, Axial-symmetric conjugated group promoting intramolecular charge transfer performances of triphenylamine sensitizers for dye-sensitized solar cells, *Dyes and Pigments* (2019), doi: https://doi.org/10.1016/j.dyepig.2019.108029.

This is a PDF file of an article that has undergone enhancements after acceptance, such as the addition of a cover page and metadata, and formatting for readability, but it is not yet the definitive version of record. This version will undergo additional copyediting, typesetting and review before it is published in its final form, but we are providing this version to give early visibility of the article. Please note that, during the production process, errors may be discovered which could affect the content, and all legal disclaimers that apply to the journal pertain.

Axial-symmetric conjugated group promoting intramolecular charge transfer performances of triphenylamine sensitizers for dye-sensitized solar cells

Shaorui Chen [a*], Juan Pei [a], Zhihan Pang [b], Wenjun Wu [b*], Xudong Yu [a], Cong Zhang [a]

[a] College of Science, Hebei University of Science and Technology, Shijiazhuang 050018, Hebei, China

[b] Key Laboratory for Advanced Materials and Institute of Fine Chemicals, East China University of Science and Technology, Shanghai 200237, China

Abstract: The intramolecular charge transport (ICT) process directly determines the charge generation, transport, and even injection of the dye-sensitized solar cell (DSSC) sensitizer. Herein, we constructed a new series of D-π-A system by linking 4-methoxyphenyl and triphenylamine donors with an ethynyl group having an axial-symmetric conjugated system. Since the axisymmetric conjugate group overcomes the reduction of the conjugate characteristic caused by the plane distortion, the molecular ICT performance and the electronic recombination inhibition are effectively improved. As a result, the photoelectric conversion efficiency was increased from 3.43% to 6.37% by means of the extension of the π-bridge at same time. It provides a new idea for the design and development of DSSC sensitizers in the future.

Key words：Triphenylamine; Dye-sensitized Solar Cells; D-π-A; ethynyl group

1. Introduction

As a result of the growing energy demand and the pollution of fossil fuels, people urgently need new energy to replace fossil energy. Dye-sensitized solar cells (DSSC), as the

* Corresponding author:

E-mail: sjz_wgq@126.com(SR Chen); wjwu@ecust.edu.cn (WJ Wu)

third-generation photovoltaic technology, have attracted considerable and sustainable attention due to their potential application as a renewable and clean energy source [1-5]. At present, the highest photoelectric conversion efficiencies (PCE) of DSSC based on ruthenium-complexes and Zn-porphyrins are 11.9% and 13%, respectively [6-7]. It is worth noting that PCE value on pure organic sensitizers over 14% under AM 1.5G irradiation [8]. Recently, SS Soni and SC Tan have reported that novel organic ionic conductors show high performances acting as a redox mediator and a light absorbing material at the same time [9-10]. As a crucial component in a typical DSSC, the dye plays an important role in the light absorption, charge separation, and electron injection [11-13]. The metal-free organic dyes have been extensively developed owing to their high molar extinction coefficients (ε), simple preparation and purification procedures, low-cost, and environmental friendly [14-15]. The development of low-cost and species abundance metal-free organic dyes to replace the expensive and source-limited ruthenium dyes is highly demanded and certainly a state of the art research topic.

Generally, metal-free organic dyes are constituted by donor (D), π-bridge (π) and acceptor (A) moieties, so called D-π-A character, which induces the intramolecular charge transfer (ICT) from subunit D to A through the π-bridge when a dye absorbs light [16-19]. Among them, introducing auxiliary groups in the skeleton of D-π-A system can exhibit a significant influence on the energy levels, light response, dye stability as well as photovoltaic performances in organic sensitizers [20-22]. Triphenylamine (TPA) dyes are widely used in DSSCs as sensitizers for their strong electron-donating ability and hole-transport properties [23-25]. Theoretical and experimental studies have demonstrated that a triphenylamine moiety can effectively suppress the dye aggregation due to its nonplanar structure and TPA-based dyes have shown promise in the

fabrication of highly efficient photovoltaic devices [26]. However, three phenyl groups of conventional triphenylamine are noncoplanar, which weakens the intermolecular electron interactions, therefore hindering the maximization of electron-donating ability [27-30]. In order to improve the cell performance, a double bond is also introduced into different positions of the π-conjugation systems to tune the molecular structure and their configurations [31]. The triple bond π-bridge has been utilized for conjugated donor-acceptor systems because it is a rigid and straight for conducting electrons and at the same time reduces charge recombination [32-34]. In addition, the introduction of triple bond could red-shift the dye's absorption spectrum due to the enhancement of the π-spacer [35-36]. However, it is rarely introduced to the donor applied into DSSC sensitizers and scrutinized the relationship between the structure of the dye and the efficiency of devices.

With this in mind, herein we develop a series of new triphenylamine dyes (**T-2** and **T-3**) (Fig. 1), in which triphenylamine linking 4-methoxyphenyl with an ethynyl group is used as electron-donating moiety, cyanoacrylic acid as electron acceptor, and ethylene or 1,3-butadiene moiety as π-conjugations to bridge the donor-acceptor (D-A) systems. Its activity as sensitizer is also compared with typical D-π-A system of **T1** and **N719**. By comparison, **T-2** and **T-3** outperform the **T-1** control one in terms of absorption properties and photovoltaic performance, indicating 4-methoxyphenyl with an ethynyl group having axisymmetric conjugate group is a promising building block for organic dyes.
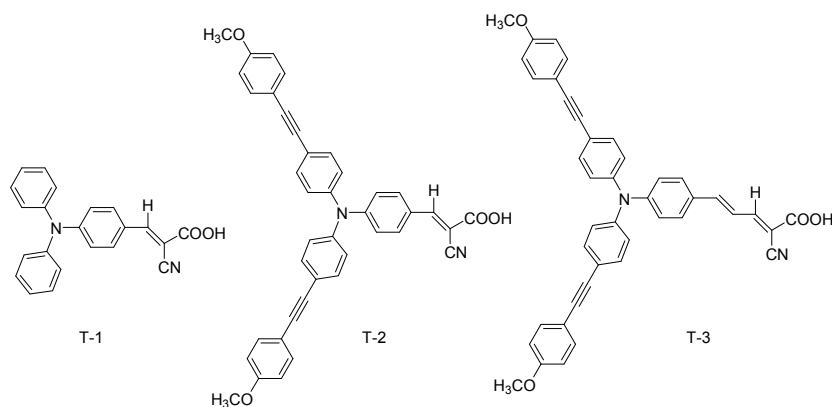
Fig. 1 Molecular structure of **T-1**, **T-2** and **T-3**.

2. Experiment

2.1 Materials and reagents

All chemicals and solvents were analytical grade and without further purification. Tertbutylpyridine (TBP), lithium iodide, and 1-methyl-3-propylimidazolium iodide (PMII) were obtained from Adamas. Transparent (18 NRT) and active opaque (18NR-AO) TiO_2 paste were obtained from Greatcellsolar Ltd (Australia). The transparent fluorine-doped tin oxide (FTO) conducting glass (fluorine-doped SnO_2, transmission > 90% in the visible range, sheet resistance 15Ω/square) was from Yingkou OPV Tech New Energy Co., Ltd. It was washed with a detergent solution, deionized water, acetone and ethanol successively under ultrasonication for 20 min before use. Thin layer chromatography purification was carried out using silica gel purchased from Qingdao Haiyang Co. LTD, China.

2.2 Instrumentation

^{1}H and ^{13}C NMR spectra were performed using Bruker 500 MHz instrument with tetramethylsilane as the internal standard. UV-vis absorption spectra were recorded on a UV-vis 2550 spectroscope (Shimadzu). Fluorescence spectra were collected on an Edinburgh instrument FLS-920 spectrometer with a Xe lamp as an excitation source. Cyclic voltammetry (CV) was

carried out on a CHI760E electrochemical workstation in CH_2Cl_2, using tetra-n-butylammonium

hexafluorophosphate as support electrolyte (10^{-1} M); scan rate: 100 mV s^{-1}. The electrochemical

cell was equipped with three electrodes: a working electrode (plate Pt electrode), an auxiliary

electrode (platinum wire electrode), and a reference electrode (Ag/AgCl electrode). Photovoltaic

measurements were performed by employing an AM 1.5 solar simulator equipped with a 300 W

Xe lamp (model no. 91160, Newport). The power of the simulated light was calibrated to 100 mW

cm^{-2} using a Newport Oriel PV reference cell system (Model 91150V). J-V curves were obtained

by applying an external bias to the cell and measuring the generated photocurrent with a Keithley

model 2400 digital source meter. The voltage step and delay time of the photocurrent were 10 mV

and 40 ms, respectively. The incident IPCE values of all DSSCs were measured by using a

Newport-74125 system (Newport Instruments). The intensity of monochromatic light was

detected by using a Si detector (Newport-71640). The EIS measurements of all DSSCs were

performed by using a Zahner IM6e Impedance Analyzer (ZAHNER-Elektrik GmbH & CoKG,

Kronach, Germany) in a frequency range of 0.1 Hz-100 kHz with an alternative signal of 5 mV at

a constant temperature of 25 □ in dark conditions.

2.3 Fabrication of DSSC

All working electrodes used in this work were prepared and modified following a reported

procedure [29]. The working electrode was composed of an 8 µm thick TiO_2 film, including a 4

µm transparent layer with 18 NRT and 4 µm scattering layer with 18NR-AO. The dye solutions

were 0.3 mM in acetonitrile and the photoanodes underwent dipping for 12 h in the dark to

complete the loading with sensitizers. The counter electrode was prepared by drop casting an

H_2PtCl_6 solution (0.02 M in 2-propanol solution) onto FTO glass and sintered under 400 °C for 15

min. The iodine electrolyte was a solution of 0.1 M LiI, 0.05 M I_2, 0.6 M 1-methyl-3-propylimidazolium iodide (PMII), and 0.5 M TBP in a mixture of acetonitrile and valeronitrile (volume ratio of 85:15). For the assemblage of DSSC, the dye-covered TiO_2 electrode and Pt counter electrode were assembled into a sandwich type cell and sealed with a hot-melt gasket of 25 μm thickness made of the ionomer Surlyn 1702 (DuPont). And then, a drop of the electrolyte was put on the hole in the back of the counter electrode. It was introduced into the cell via vacuum backfilling. The hole in the counter electrode was sealed by a film of Surlyn 1702 and a cover glass (0.1 mm thickness) using a hot press. The size of the TiO_2 electrodes used was 0.25 cm^2 (i.e. 5 mm × 5 mm). In this work, all test data shown were the average values of five parallel tests.

2.4 Synthesis of dyes

N, N-dimethylformamide (DMF) were distilled with CaH_2. **T-1** was conveniently synthesized according to the literature method [37]. Other chemicals and reagents were purchased from commercial suppliers without further purifications. The synthetic route of **T-2** and **T-3** are shown in **Scheme 1**.
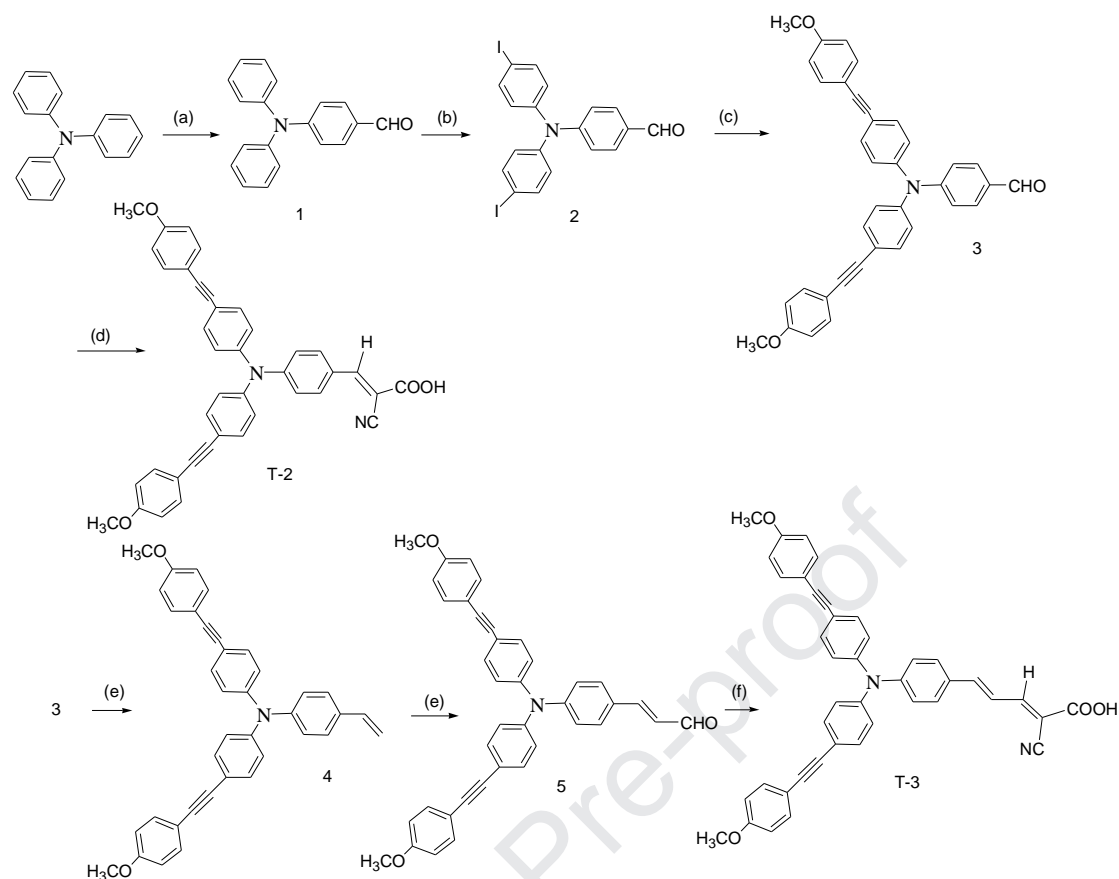
Scheme 1. Synthesis of dyes **T-2** and **T-3**

(a) POCl$_3$, DMF, 80 □, 8 h, 86%; (b) potassium iodide, I$_2$, 60 □, 12h, 75%; (c) Pd(II), copper iodide, P(Ph)$_3$, K$_3$PO$_4$, 110 □, 17 h, 72%; (d) cyanoacetic acid, piperidine, acetonitrile, reflux, 8 h, 51%; (e) P(Ph)$_3$CH$_3$Br, Potassium *t*-Butoxide, rt, 2h, 97%; (f) POCl$_3$, DMF, 80 □, 12 h, 81% ; (g) cyanoacetic acid, piperidine, acetonitrile, reflux, 10 h, 55%.

2.4.1 synthesis of 4-(N,N-diphenylamino)benzaldehyde (*1*)

phosphorous oxychloride (POCl$_3$) (3.29 g, 21.5 mmol) was added dropwise to the mixture of triphenylamine (4.9 g, 0.02 mmol) and N, N-dimethylformamide (40 mL) at 25 □. The reaction mixture was stirred and heated at 80 □ for 8 h. After cooling down to room temperature, the reaction mixture was poured into 50 mL cold water and acidized with dilute hydrochloric acid and extracted with dichloromethane (50 mL × 3). The combined organic layer was dried with anhydrous MgSO$_4$, filtered and evaporated under reduced pressure. The residue was purified by column chromatography on silica gel and eluted with petroleum ether/ethyl acetate to afford

compound **1** (4.72 g, 86 %) as a pale yellow solid. m.p. 128-130 □ (lit. [38] 129-133 □); ^{1}H NMR

(500 MHz, CDCl$_3$) δ (ppm): 7.03 (d, *J* = 8.8 Hz, 2H, Ph), 7.17-7.19 (m, 6H, Ph), 7.34 (t, *J* = 8.0

Hz, 4H, Ph), 7.69 (d, *J* = 8.8 Hz, 2H, Ph), 9.81 (s, H, -CHO).

2.4.2 synthesis of 4-[N,N-di(4-iodophenyl)amino]benzaldehyde (2)

The mixture of compound **1** (1.36 g, 4.98 mmol), 1.58 g (6.22 mmol) iodine and 40 mL

ethanol were heated to 60 □ and stirred for 30 min, then the solution of iodic acid (0.88 g, 5

mmol) in water (5 mL) were added dropwise. The reaction was stirred at 60 □ in nitrogen for 12h.

The solution was allowed to cool and the solid was collected, washed with ethanol and

recrystallised with CH$_2$Cl$_2$-ethanol giving the product (1.84 g, 75 %). m.p. 147.0-148.5 □ (lit. [39]

148.0 -150.0 □); ^{1}H NMR (500 MHz, DMSO, Fig. S1) δ (ppm): 6.95 (d, *J* = 8.5 Hz, 4H, Ph), 7.00

(d, *J* = 8.5 Hz, 2H, Ph), 7.71 (d, *J* = 8.5 Hz, 4H, Ph), 7.76 (d, *J* = 9.0 Hz, 2H, Ph), 9.82 (s, H,

-CHO).

2.4.3 synthesis of 4-(N,N-bis(4-((4-methoxyphenyl) ethynyl)phenyl)amino) benzaldehyde (3)

Under N$_2$ atmosphere, compound **2** (0.52 g, 0.99 mmol), copper (I) iodide (0.076 g, 0.04

mmol), dichlorobis (triphenylphosphine) palladium (II) (0.026 g, 0.04 mmol), triphenyl phosphine

(0.01 g, 0.04 mmol), potassium phosphate (1.2 g, 5.66 mmol), and 4-methoxyphenyl acetylene

(0.34 g, 2.5 mmol) were dissolved in dry DMF (15 mL). The reaction was then heated at 110 □

for 17 h, then was quenched with water and extracted with CH$_2$Cl$_2$. The organic layer was dried

with anhydrous MgSO$_4$. Silica gel chromatography with petroleum ether/dichloromethane gave

compound **3** with the yield of 72 % (0.37 g). m.p. 183.8 -185.7 □; ^{1}H NMR (500 MHz, CDCl$_3$,

Fig. S2) δ (ppm): 3.83(s, 6H, -OCH$_3$), 6.88 (d, *J* = 8.5 Hz, 4H, Ph), 7.10-7.12 (m, 8H, Ph), 7.46 (d,

J = 7.5 Hz, 6H, Ph), 7.73 (d, *J* = 8.5 Hz, 2H, Ph), 9.86 (s, H, -CHO); ESI-MS (m/z): 534.3 (M +

H)$^+$; Anal. Calcd. for $C_{37}H_{27}NO_3$, %: C 83.28; H 5.10; N 2.62; Found C 83.27; H 5.35; N 2.76.

2.4.4 synthesis of 3-(4-(4-(bis(4-((4-methoxyphenyl)ethynyl)phenyl)amino)phenyl) -2- cyanoacrylic

acid (T-2)

To a stirred solution of compound **3** (0.20 g, 0.37 mmol) in 10 mL of acetonitrile, cyanoacetic

acid (0.061 g, 0.72 mmol) and piperidine (3-5 drops) were added. The mixture was heated to

reflux for 9 h. After cooling, the reaction mixture was diluted with dichloromethane (20 mL),

washed with water (20 mL) and hydrochloric acid (20%, 20 mL). The organic layer was separated,

dried with $MgSO_4$ and concentrated in a rotary evaporator to get crude **T-2.** The crude product was

purified by column chromatography (methanol/dichloromethane as eluent) to afford **T-2** as red

solid. Yield 51 %, 0.12 g; m.p.153.3 -154.7 □; ^{1}H NMR (500 MHz, CDCl$_3$, Fig. S3) δ (ppm):

3.84(s, 6H, -OCH$_3$), 6.88 (d, *J* = 8.5 Hz, 4H, Ph), 7.08 (d, *J* =9.0 Hz, 2H, Ph), 7.12 (d, *J* = 8.5 Hz,

4H, Ph), 7.46-7.49 (m, 8H, Ph), 7.91 (d, *J* = 8.5 Hz, 2H, Ph), 8.16 (s, H,-CH=); ^{13}C NMR (125

MHz, CDCl$_3$, Fig. S4) δ (ppm): 58.13, 90.29, 92.95, 116.87, 118.03, 123.42, 123.49, 127.18,

128.54, 135.73, 135.87, 147.73, 154.71, 157.85, 162.52; ESI-MS (m/z): 601.3 (M + H)$^+$; Anal.

Calcd. for $C_{40}H_{28}N_2O_4$, %: C 79.98; H 4.70; N 4.66; Found C 80.27; H 4.55; N 4.76.

2.4.5 synthesis of 4-(N,N-bis(4-((4-methoxyphenyl) ethynyl)phenyl)amino) styrene (4)

Under N$_2$ atmosphere, potassium tert-butanol (*t*-BuOK) (0.43g, 3.84mmol) was added into 70

mL THF solution. After stirring for 30 minutes, *t*-BuOK was completely dissolved and the mixture

was cooled to 0 □. Methyl triphenylphosphonium bromide (1.20 g, 3.84 mmol) and compound **3**

(0.64 g, 1.19 mmol) were added. The reaction mixture was stirred for another 2 h at room

temperature, and then poured into ice water mixture followed by extraction with dichloromethane.

The organic layer was dried over $MgSO_4$. After evaporation of solvent, the crude product **4** was

obtained. The crude product was purified by column chromatography petroleum ether/ dichloromethane as eluent to afford compound **4** as white solid. Yield 97 %, 0.62 g; m.p. 193.0 -194.7 □; ^{1}H NMR (500 MHz, CDCl$_3$, Fig. S5) δ (ppm): δ: 3.85 (s, 6H, -OCH$_3$), 5.22 (d, J = 11.0 Hz, 1H, = CH$_2$), 5.71 (d, J = 17.5Hz, 1H, = CH$_2$), 6.68 (dd, J_1 = 17.5 Hz, J_2 = 11.0 Hz, 1H, -CH=C), 6.86 (d, J = 8.5 Hz, 4H, Ph), 7.04 (d, J = 11.0 Hz, 6H, Ph), 7.33 (d, J = 8.5 Hz, 2H, Ph), 7.38 (d, J = 8.5 Hz, 4H, Ph); ^{13}C NMR (125 MHz, CDCl$_3$, Fig. S6) δ (ppm): 55.34, 88.05, 89.04, 112.98, 114.03, 115.62, 117.76, 123.60, 124.91, 127.34, 132.97, 133.24, 136.09, 146.37, 146.81, 159.53; ESI-MS (m/z): 532.3 (M + H)$^+$; Anal. Calcd. for C$_{38}$H$_{29}$NO$_2$, %: C 85.85; H 5.50; N 2.63; Found C 85.77; H 5.75; N 2.76.

2.4.6 synthesis of 4-(N,N-bis(4-((4-methoxyphenyl) ethynyl)phenyl)amino) phenyl) acrylaldehyde

(5)

At room temperature, phosphorous oxychloride (POCl$_3$) (1.2 mL) was added dropwise to dry N, N-dimethylformamide (10 mL). The mixture stirred for 1 h and compound **4** (0.67 g, 1.26 mmol) was added. Then the reaction mixture still stirred for another 12 h and was adjusted to be neutral using 20% NaOH aqueous solution, extracted with CH$_2$Cl$_2$. The organic layer was dried with anhydrous MgSO$_4$. Silica gel chromatography with petroleum ether/dichloromethane gave compound **5** with the yield of 81 % (0.56 g). m.p. 163.8-165.5 □; ^{1}H NMR (500 MHz, CDCl$_3$, Fig. S7) δ (ppm): 3.85 (s, 6H, -OCH$_3$), 6.67 (d, J = 8.5 Hz, 4H, Ph), 7.11 (d, J = 8.5 Hz, 6H, Ph), 7.48 (d, J = 7.5 Hz, 8H, Ph), 7.72 (d, J = 8.5 Hz, 2H, Ph), 9.85 (s, 1H, -CHO); ^{13}C NMR (125 MHz, CDCl$_3$, Fig. S8) δ (ppm): 55.35, 87.71, 89.65, 114.06, 119.30, 122.85, 124.83, 126.83, 128.18, 129.93, 132.78, 133.03, 149.73, 152.16, 159.66, 193.62; ESI-MS (m/z): 560.4 (M + H)$^+$; Anal. Calcd. for C$_{39}$H$_{29}$NO$_3$, %: C 83.70; H 5.22; N 2.50; Found C 83.77; H 5.25; N 2.66.

2.3.7 synthesis of (2E,4E)-5-(4-(4-(bis(4-((4-methoxyphenyl)ethynyl)phenyl)amino)phenyl)-2-cyano-2,

*4-pentadienoic acid (**T-3**)*

The mixture of compound **5** (0.20 g, 0.36 mmol) cyanoacetic acid (0.061 g, 0.72 mmol) and

piperidine (3-5 drops) in 10 mL of acetonitrile was heated to reflux for 9 h, poured into 20 mL

water, extracted with dichloromethane, dried with $MgSO_4$ and concentrated in a rotary evaporator

to get crude **T-3.** The crude product was purified by column chromatography (methanol /

dichloromethane as eluent) to afford **T-3** as red solid. Yield 55 %, 0.13 g; m.p.127.3 -128.7 □; [1]H

NMR (500 MHz, $CDCl_3$, Fig. S9) δ (ppm): 3.86 (s, 6H, $-OCH_3$）, 6.85 (d, *J* = 9.0 Hz, 4H, Ph),

7.06-7.10 (m, 6H, Ph), 7.20 (s, 1H, -CH=C), 7.23 (s, 1H, =C-CH), 7.44-7.49 (m, 10H, Ph), 8.02 (d,

J = 11.0 Hz, 1H, -C=CH); ^{13}C NMR (125 MHz, $CDCl_3$, Fig. S10) δ (ppm): 55.33, 87.66, 89.77,

101.73, 114.04, 115.34, 119.57, 121.13, 122.47, 125.02, 128.58, 130.30, 132.79, 133.02, 145.67,

149.46, 149.96, 157.07, 159.64, 166.96; ESI-MS (m/z): 627.3 (M + H)[+]; Anal. Calcd. for

$C_{40}H_{30}N_2O_2$, %: C 80.49; H 4.82; N 4.47; Found C 80.57; H 4.98; N 4.66.

3. Results and discussion

3.1. Synthesis and characterization

Two dyes **T-2** and **T-3** were synthesised from triphenylamine as the starting material.

Compound **1** was synthesized according to the literature [38]. 4-[N, N-di (4-iodophenyl) amino]

benzaldehyde was obtained using iodine and iodic acid in the solution of ethanol. While using

potassium iodide and potassium iodate, the structure of target compound is not correct by NMR

spectra [40]. Then the solution of Sonogashira coupling was employed to attach

4-methoxyphenylethynyl group to the compound **2** [41]. On the one hand, the aldehyde was

converted to cyanoacetic acid derivatives (**T-2**) by refluxing with cyanoacetic acid in the presence

of piperidine in dry acetonitrile [42]. On the other hand, a Wittig reaction between phosphonium

salt and compound **3** gave styrene derivative **4** [43]. Using Vilsmeier-Haack reaction, compound **5**

was obtained, which in turn was condensed with cyanoacetic acid to give dye **T-3** in good yield.

The proposed structures of all the final compounds were confirmed using characterization

techniques such as NMR, MS and elemental analysis spectroscopies.

3.2. Photophysical properties

The UV-vis absorption for **T-1, T-2** and **T-3** in dilute solutions of CH_2Cl_2 $(1.67 \times 10^{-5}$ M) are

presented in Fig. 2a and the corresponding data are summarized in Table 1. All of the dyes with a

strong absorption maximum in the visible region corresponding to the highest occupied molecular

orbital (HOMO) to the lowest unoccupied molecular orbital (LUMO) transitions are observed [44].

The absorption spectrum of **T-1** shows an absorption maximum (λ_{max}) at 434 nm (36200 $M^{-1}cm^{-1}$).

Compared to **T-1**, the absorption spectrum of **T-2** shows two absorption maxima at 358 nm (62600

$M^{-1}cm^{-1}$) and 430 nm (41000 $M^{-1}cm^{-1}$). Both of the width and intensity of the absorption peak for

T-2 (430 nm) are bigger than those of **T-1**. Introduction of 1, 3-butadiene moiety as π-bridge to

T-2, giving **T-3**, causes a further red shift to 460 nm (35400 $M^{-1}cm^{-1}$). This result suggested that

the introduction of 4-methoxyphenyl with ethynyl group having axisymmetric conjugate group to

the donor was beneficial to red shift the charge-transfer transition. Theoretical computation shows

that the ground state structure of **T-1** possesses a 50.2° twist between the diphenylamine and the

phenyl ring, and the dihedral angle in **T-2** is 49.2° because of the introduction of 4-methoxyphenyl

with ethynyl group, giving less twist than that of **T-1**. Furthermore, the dihedral angle in **T-3** is

45.3° (Table 2). Introducing 4-methoxyphenyl with ethynyl group and double bond, giving **T-3**,

causes the largest red shift to 460 nm because of not only enhancement of the electron-donating

ability of the TPA donor but also the best delocalization over an entire conjugated system in **T-3**

[45]. It should be noted that the red-shift usually endows the dye a wider photoresponding range,

which is favorable for light harvesting and photocurrent generation in DSSC.
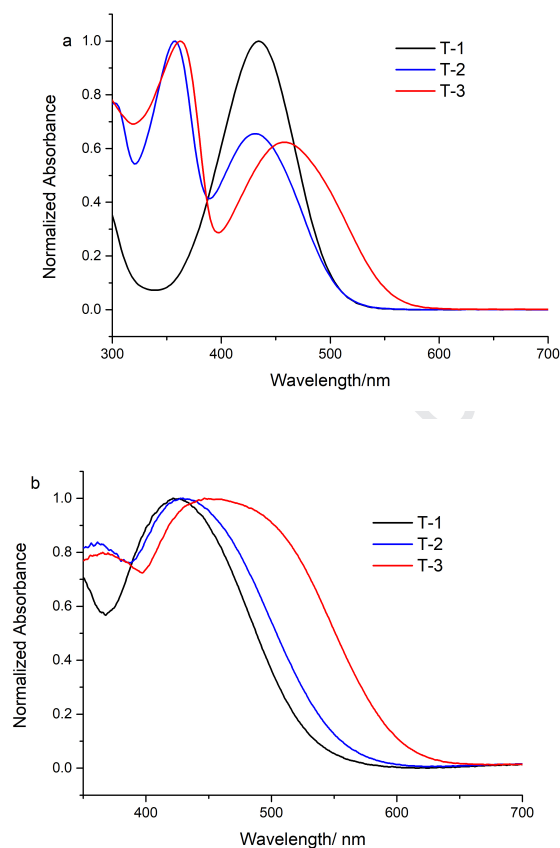
Fig. 2 Absorption spectra of dyes **T-1**, **T-2** and **T-3** measured in CH_2Cl_2 (**a**) and adsorbed onto 4 μm transparent TiO_2 films (**b**).

Table 1 Photophysical and electrochemical properties for **T-1**, **T-2** and **T-3**

Dyes	λ_{max} [a]	ε [b]	λ_{max} [c]	λ_{em} [d]	λ_{inset} [e]	E_{0-0} [f]	E_{ox} [g]	E_{red} [h]	Dye loading amount [I]
	nm	$M^{-1}cm^{-1}$	nm	nm	nm	V	V	V	$(mol\ cm^{-2})$
T-1	434	36200	422	521	463	2.68	1.18	-1.50	2.06×10^{-7}
T-2	430	41000	428	538	468	2.65	1.19	-1.46	2.08×10^{-7}
T-3	460	35400	457	595	502	2.47	0.95	-1.52	2.73×10^{-7}

Note:

[a] Absorption parameters were obtained in CH_2Cl_2.

[b] The molar extinction coefficient at λmax in CH_2Cl_2 solution.

[c] Absorption parameters were obtained on 4 μm nanocrystalline TiO_2 film.

[d] Emission maximum in CH_2Cl_2 solution.

[e] The intersection of normalized absorption and emission spectra.

[f] Obtained from the intersection between the absorption and emission spectra $E_{0-0} = 1240/\lambda_{inse}$ (Fig.S11).

[g] The oxidation potentials of the dyes were measured in CH_2Cl_2 solutions with ferrocene/ferrocenium (Fc/Fc^+) as an external reference and

converted to NHE.

[h] The E_{red} was calculated according to $E_{red} = E_{ox} - E_{0-0}$.

[I] The dye loads are calculated from absorbance data of the sensitized TiO_2 electrodes.

Table 2 Optimized Conformations Calculated with Gaussian 09 program package of the Selected Dyes

T-1 structure	**T-2** structure	**T-3** structure
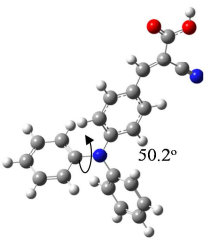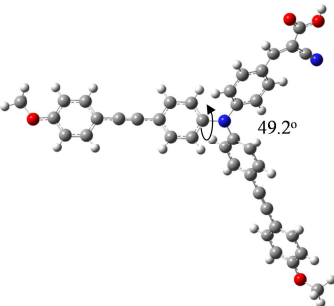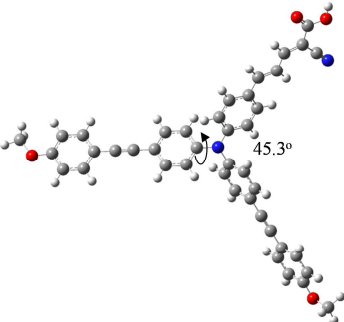
The UV-vis absorption spectra for the dye-loaded TiO_2 film (4 μm) are shown in Fig. 2b. The

onset points of the absorption spectra are about 530 nm for **T-1**, 560 nm for **T-2**, 610 nm for **T-3**.

After being absorbed on TiO_2 nanoparticle films, the absorption band of **T-3** is broader by 50 nm

than that of **T-2** and **T-2** is broader by 30nm than that of **T-1**. Such bathochromic shift of the

absorption spectrum is due to the introduction of axial-symmetric conjugated group

(4-methoxyphenyl with ethynyl group) and the longer π-bridge. The absorption ranges of the three

dyes are all broadened to different degrees after anchoring on TiO_2 nanoparticle film. The TiO_2 surfaces play an important role in organizing and orienting the adsorbed dye molecules. The broadening of the absorption spectrum of the three dyes on TiO_2 might be due to dye-TiO_2 interactions, dye-dye interactions, or both of them [46-47]. In general, strong interactions between the adsorbed dye molecules and the TiO_2 surface are known to lead to aggregate formation, thus anchoring monolayer dyes onto the TiO_2 surface and accomplishing higher solar energy conversion efficiency of DSCC [48].

3.3. Electrochemical properties

Cyclic voltammetry (CV) was also performed to study electrochemical properties of **T-1**, **T-2** and **T-3** as well as to estimate their feasibility of electron injection from electronically excited dyes into the conduction band of TiO_2 and dye regeneration by redox electrolytes. CV was carried out in CH_2Cl_2 solution (Fig. 3) and the relevant data was listed in Table **1**. The ground and excited states of the dyes were positioned at energy levels that have sufficient driving force for both regeneration and electron injection as shown in Scheme **2**. All redox potentials are converted on the NHE scale. The E_{red} of **T-1**, **T-2** and **T-3** are -1.50, -1.46 and -1.52V vs. NHE, respectively, which is more negative than the conducting band (CB) of TiO_2 (- 0.5 V vs. NHE), indicating that the excited state of dyes **T-1**, **T-2** and **T-3** could effectively inject electrons into the CB of TiO_2 [49]. Moreover, the ground-state oxidation potentials (E_{ox}) of **T-1**, **T-2** and **T-3** are 1.18, 1.19 and 0.95 V *vs*. NHE, respectively and more positive than the redox potentials of I^-/I_3^- (0.4 V *vs*. NHE), ensuring ample driving force for dye regeneration [50]. The introduction of 4-methoxyphenyl with ethynyl group to triphenylamine (**T-1**) promotes a little decrease in the oxidation potentials. E_{ox} value of **T-3** is significant higher compared with that of **T-1** and **T-2** due to the change of π-bridge,

leading to a better regeneration of the dye after electron injection into the conduction band of TiO$_2$.

Thus, **T-3** can undergo the charge transfer easily with high coplanarity and higher E$_{ox}$ and this

might be part of the reason why **T-3**-based DSSC exhibited the best photovoltaic performances

[51-52]. Therefore **T-1, T-2** and **T-3** are qualified to be used in DSSC in theory.
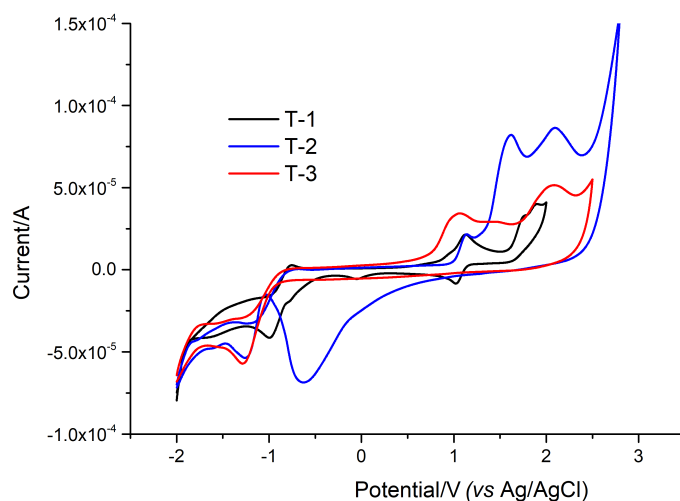
Fig. 3 Cyclic voltammograms of the dyes recorded for CH$_2$Cl$_2$ solutions (10^{-3}M) with TBAPF$_6$ (0.1 M) as the electrolyte (working

electrode: plate Pt; reference electrode: Ag/Ag$^+$; an auxiliary electrode: platinum wire; calibrated with Fc/Fc$^+$ as an internal reference;

scan rate: 100 mV s^{-1}).
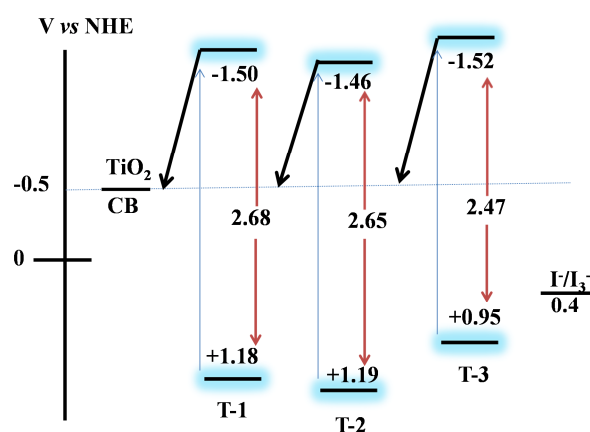
Scheme 2. Representation of HOMO and LUMO levels of **T-1**, **T-2** and **T-3** dyes (Potential vs. NHE).

3.4. Theoretical calculation

In order to further understand the structural properties of the dyes and the possibility of

charge transfer from donor to acceptor on electronic excitation, the electronic structure of the dyes was analyzed by density functional theoretical (DFT) calculations using the Gaussian 09 program package [53]. We optimized the molecular structure of **T-1, T-2** and **T-3** in the *vacuo*. The electron densities of HOMO and LUMO of the dyes are shown in Table 3. It is clearly that the HOMOs are delocalized between the donor and π-bridge. In the LUMO state, the electrons are mainly delocalized over the sectional π-bridge and anchoring group. The well separation of electron at HOMO and LUMO levels indicates the electron can efficiently transfer from the donor part to the acceptor part once excited, consequently giving fast electron injection from the LUMO of dyes to the CB of TiO_2. It is known that the geometry of acetylene is straight line shaped due to the sp hybridization of the C atom and the electron cloud of p-orbitals distributes in a cylindrical shape. As presented in Table 3, the axial-symmetric conjugated ethynyl group can effectively offset the reduction of the conjugation effect caused by the stereoscopic effect and promote the effective intramolecular charge transfer process.

We can also see from Table 1 and Scheme 2 that the introduction of 4-methoxyphenyl with ethynyl group to triphenylamine or the longer π-bridge could change HOMO-LUMO energy gaps of the dyes more narrowly resulting from the enhancement of molecular planar configurations with axial-symmetric distribution of π-electron in acetylene and expansion of π-bridge.

Table 3 HOMO and LUMO of the dyes **T-1**, **T-2** and **T-3** calculated with DFT method

Dye	HOMO	LUMO
T-1		
T-2		
T-3		
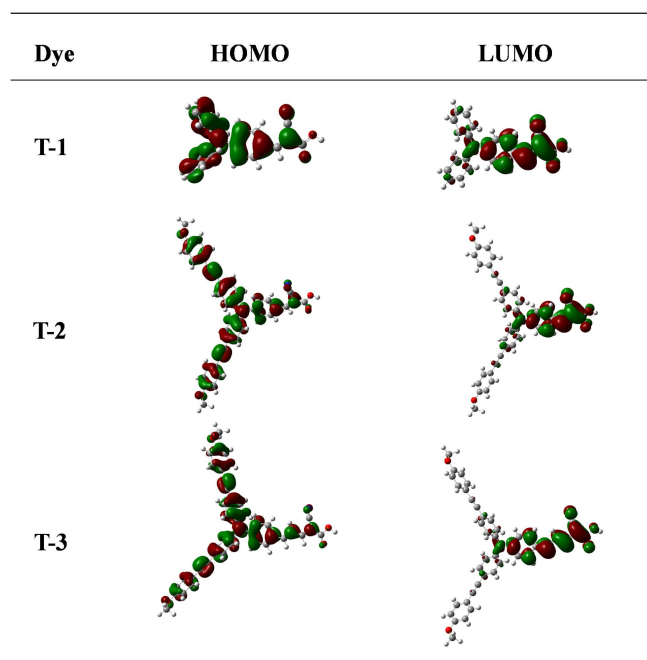
3.5. Photovoltaic performance of DSSC

These molecules **T-1**, **T-2** and **T-3** have the potential to act as light harvesting dyes for DSSC

and the *J-V* and incident photon-to-current conversion efficiency (IPCE) plots obtained are shown

in Fig.4 and Fig.5. The measured photovoltaic parameters are summarized in Table 4.

Table 4 Photovoltaic parameters of the *J-V* curves for the DSSC under irradiation of AM 1.5G sunlight.

Dyes	J_{SC} mAcm^{-2}	V_{OC} mV	FF (%)	PCE (%)
T-1	7.47 ($\pm$ 0.14)	643($\pm$ 3.23)	71.43($\pm$ 0.09)	3.43($\pm$ 0.02)
T-2	8.95($\pm$ 0.21)	700($\pm$ 2.45)	72.08($\pm$ 0.05)	4.52($\pm$ 0.02)
T-3	12.21($\pm$ 0.19)	732($\pm$ 2.79)	71.73($\pm$ 0.09)	6.37($\pm$ 0.03)

Under standard global AM 1.5 solar simulator condition (100 mW cm^{-2}), a power conversion

efficiency (PCE) of 3.43% was obtained for DSSC based on control dye **T-1** (J_{SC} = 7.47 mA/cm^2,

V_{OC} = 643 mV and FF = 71.43 %). Moreover, DSSCs fabricated using **T-2** and **T-3** sensitized cells

gave J_{SC} of 8.95, 12.21mA/cm^2, V_{OC} of 700, 732 mV and FF of 72.08, 71.73 %, corresponding to

PCE of 4.52% and 6.37%, respectively. Under the same fabrication conditions, the standard **N719** dye showed an efficiency of 8.62%. As depicted in table 4, the PCE of **T-2** reaches the maximum value of 4.52%, which is 31.8% higher than that of **T-1** (3.43%), demonstrating that the photovoltaic performance is improved after introducing 4-methoxyphenyl with ethynyl group to **T-1**. The PCE of **T-3** (6.37%) is the highest among these three dyes because of the largest V_{OC} and J_{SC}. The wide gaps between the V_{OC} and J_{SC} of **T-3**, **T-2** and **T-1** are also partially attributed to the different ability to prevent dark current as proved by Fig. 4 [54]. On the other hand, with the appearances of 4-methoxyphenyl with ethynyl group and longer of π-bridge, the dihedral angles in **T-2** and **T-3** are 49.2° and 45.3°, respectively. Better molecular planar configurations, axial-symmetric distribution of π-electron in acetylene and expansion of π-bridge of **T-3** than that of **T-2** leads to broadening absorption spectrum and thus higher J_{SC} was got for DSCC sensitized by **T-3**.

Fig.**5** shows the IPCE as a function of excitation wavelength. The onset of the IPCE spectrum of the devices based on **T-1, T-2 and T-3** is at 532 nm, 569 nm and 610 nm, respectively. It is impressive that **T-2** bestows very broader and higher IPCE values than **T-1**, while introducing 4-methoxyphenyl with ethynyl group to **T-1**. The IPCE value of **T-2** exceeds 70% from 360 to 510 nm, with the highest value (82%) at 410 nm. Compared with **T-2**, dye **T-3** shows an obviously broader response range (exceed 60% in 350-540 nm) with a maximum value of 74% at 490 nm. Although the maximum IPCE values for **T-3** was lower, its photoresponse range is much broader than that of **T-2**, resulting in a much higher J_{SC} for **T-3** based DSCC. As seen in Table 1, the dye loading amounts of **T-1**, **T-2** and **T-3** are 2.06×10^{-7}, 2.08×10^{-7} and 2.72×10^{-7} mol cm^{-2}, respectively, and the adsorption amount are calculated from absorption data in Figure 2 [55]. The

measured number of the dyes loading on TiO_2 is in the order of **T-1** < **T-2** < **T-3**, in according with those of IPCE spectra and J_{SC} values determined experimentally. The increased IPCE values of **T-2** and **T-3** relative to that of **T-1** are also attributed to the introduction of axial-symmetric conjugated group to triphenylamine or the longer π-bridge, which is in agreement with the absorption spectra of the dyes on TiO_2 films.
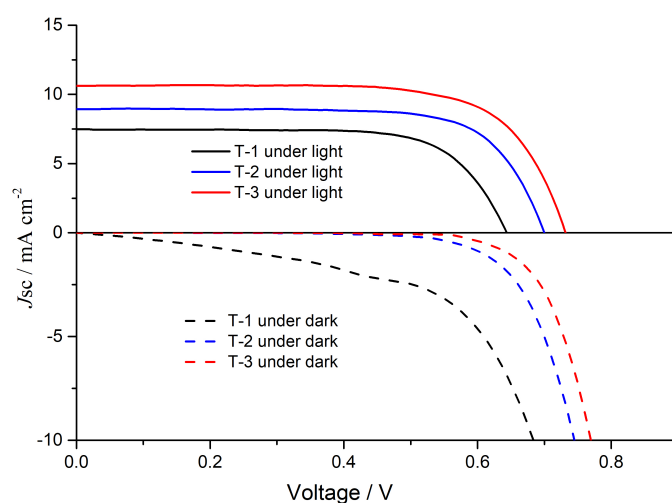
Fig. 4 *J-V* characteristics of solar devices based on **T-1**, **T-2** and **T-3**
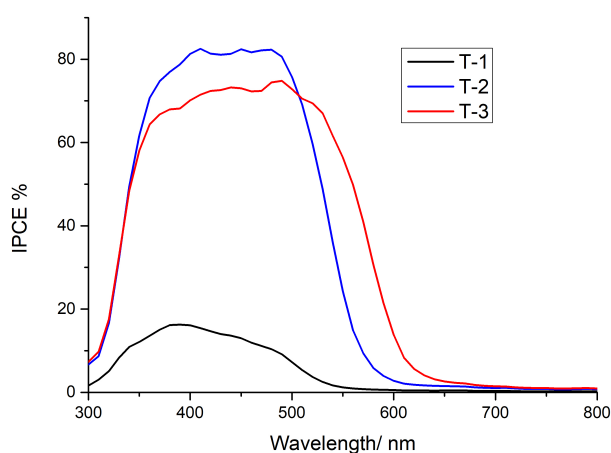
Fig. 5 Photocurrent action spectra (IPCE) of solar devices based on **T-1**, **T-2** and **T-3**

As known, the alternation of photovoltage V_{OC} originates from the displacement of quasi□Fermi□level (E_f) in TiO_2, which intrinsically stems from the change of TiO_2 conduction

band edge (E_{CB}) and/or fluctuation of electron density (charge recombination rate in DSSC) with same electrolyte [56]. In order to determine the energy levels of the electrode sensitized by different dyes, electrochemical impedance spectroscopy (EIS) was performed on **T-1**, **T-2** and **T-3** and shown in Fig. **6**. As presented in Fig**. 6a**, the chemical capacitance (C_μ) of **T-2** or **T-3** was increased linearly with the given bias potential, and all the curves exhibited the same slope. At fixed potential close to their V_{OC} (e.g. 0.70V), the order of C_μ is **T-2 > T-3 > T-1**. Due to the density of occupied state (DOS) which is proportional to C_μ increases with the downward shift of the TiO$_2$ conduction band, the C_μ is inversely proportional to the position of the conduction band [57]. Therefore, the position of the conduction band partially determines the size of the open circuit voltage. C_μ of **T-2** is higher than that of **T-3**, ruling out the downward shift of the conduction band shift as the main reason for the decreased V_{OC} for **T-2**. To take insight into the electron recombination occurring between excited electrons in conduction band with sensitizers or electrolyte, the electron lifetime was tested as a function of potential bias. At a given potential, the electron lifetime in cell sensitized with **T-3** was obviously the longest with iodine electrolyte (Fig. **6b**), while **T-1** got the shortest one, which is exactly consistent with the sequence of V_{OC}. The significant increase in electron recombination lifetime means that the charge recombination arising from electrons in TiO$_2$ CB with the I$_3^-$ ion in electrolyte is suppressed by the introduction of the 4-methoxyphenyl with ethynyl group and longer π-bridge, and the ICT process was promoted with the help of axial-symmetric electrons in ethynyl group. Thus, we can conclude that introduction of 4-methoxyphenyl with ethynyl group and the extension of the π-bridge based on **T-1** as the primary sensitizer, the charge recombination could be repressed effectively, and the devices could succeed superior V_{OC} performance from **T-1** to **T-3** [58].
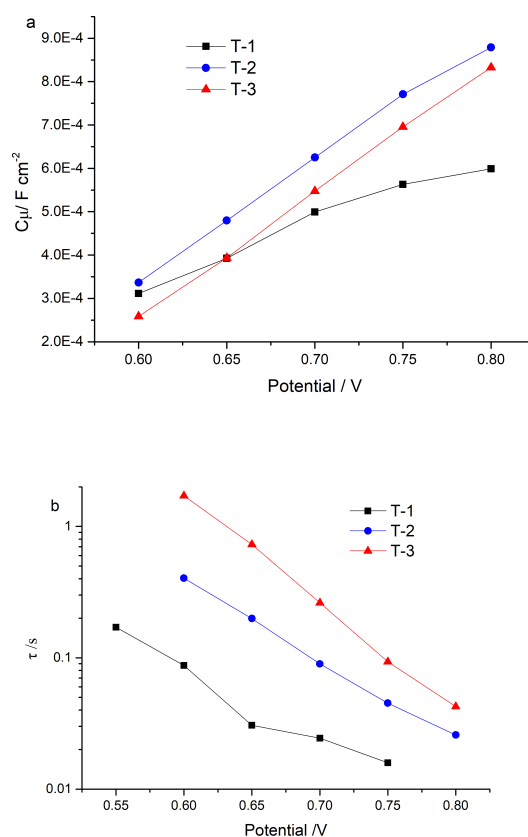
Fig.6. Chemical capacitance (a) and electron lifetime (b) as a function of bias potential obtained through electrochemical impedance spectroscopy

carried on devices with iodine electrolyte.

The stability of **T-1**, **T-2** and **T-3** sensitized photovoltaic devices were investigated by storing at

room temperature and 40-60% humidity. As shown in Fig. 7, for **T-1**, **T-2** and **T-3**, the

photoelectric conversion efficiency was approximately 67%, 78% and 86% of the initial value,

respectively, after 10 days. It is indicated that the introduction of the alkynyl group into donors for

T-2 and **T-3** and the expansion of conjugated bridge for **T-3** can effectively improve the

photothermal stability of the sensitizers. Especially for **T-3**, after a short degradation in the first

three days, then the PCE stabilized for a longer period of time. By tracking their V_{OC} and J_{SC}, it

was found that J_{SC} is the determinant factor for the degradation of the PCE due to their almost

same variation tendency. The decrease in current density maybe related to the photo degradation

of trace dye. This stability test also provides a theoretical guidance for our future structural design.
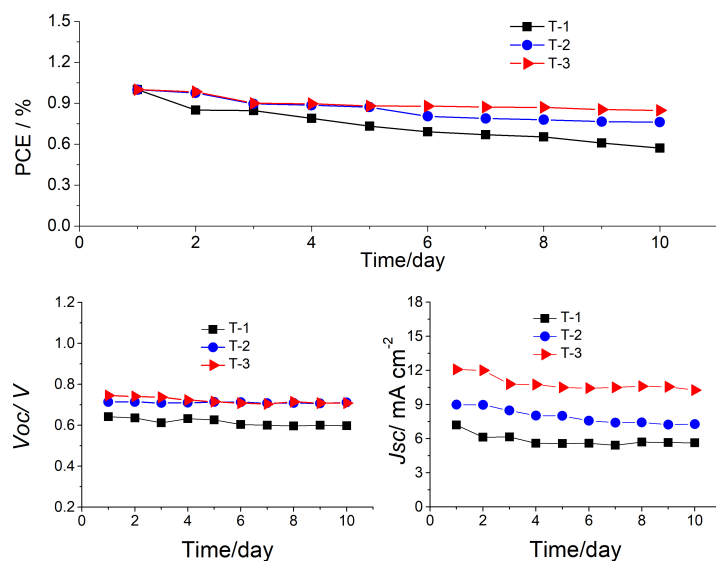
Fig. 7 Stability test showing the variation in the photovoltaic parameters (Normalized PCE, V_{OC}, and J_{SC}) with ageing time for devices with **T-1**, **T-2**

and **T-3** and with PCBM treatment (red line) under room temperature and 40–60% humidity.

4. Conclusions

In summary, two novel metal-free organic dyes with ethynyl group having an axial-symmetric conjugated system, named **T-2** and **T-3** were synthesized and applied in DSCC. Introduction of the 4-methoxyphenyl with ethynyl group and the extension of π-bridge to **T-1**, the decrease of dihedral angles between the benzene and diphenylamine increase the coplanar property between donor and π-bridge, which is in favor of the intermolecular charge transfer. The absorption spectra, short-circuit photocurrent densities (J_{SC}) and open-circuit photovoltages (V_{oc}) were improved to a large extent. Under AM 1.5G irradiation, the energy conversion efficiencies of DSSCs based on **T-3** and **T-2** are up to 6.37% and 4.52% respectively. Electrochemical impedance spectroscopy (EIS) analysis reveals that the introduction of the 4-methoxyphenyl with ethynyl group or the extension of π-bridge could suppress the charge recombination arising from electrons in TiO$_2$ film and the I$_3^-$ ion in electrolyte and promote the ICT process, thus improving the V_{OC} of

DSCC considerably. This study provides useful information for further design and synthesis of DSSC sensitizers.

Acknowledgments

References

[1] Chen C, Cheng M, Ding XD, Li HP, Qiao F, Xu L, Li HN, Li HM. Molecular engineering of triphenylamine functionalized phenoxazine sensitizers for highly efficient solid-state dye sensitized solar cells. Dyes Pigments 2019; 162: 606-10.

[2] Dai PP, Yang L, Liang M, Dong HH, Wang P, Zhang CY, Sun Z, Xue S. Influence of the Terminal Electron Donor in D-D-π-A Organic Dye-Sensitized Solar Cells: Dithieno [3,2-b:2′,3′-d]pyrrole versus Bis(amine). ACS Appl Mater Inter 2015; 7: 22436-47.

[3] Cheng H, Wu YG, Su JY, Wang ZH, Ghimire RP, Liang M, Sun Z, Xue S. Organic dyes containing indolodithienopyrrole unit for dye-sensitized solar cells. Dyes Pigments 2018; 149: 16-24.

[4] Wang YQ, Li X, Liu B, Wu WJ, Zhu WH, Xie YS. Porphyrins bearing long alkoxyl chains and carbazole for dye-sensitized solar cells: tuning cell performance through an ethynylene bridge. RSC Adv 2013; 3: 14780-90.

[5] Wang YQ, Xu L, Wei XD, Li X, Ågren H, Wu WJ, Xie YS. 2-Diphenylaminothiophene as the donor of porphyrin sensitizers for dye-sensitized solar cells. New J Chem 2014; 38: 3227-35.

[6] Nazeeruddin MK, Kay A, Rodicio I, HumpbryBaker R, Miiller E, Liska P, Vlachopoulos N, Graetzel M. Conversion of light to electricity by cis-X$_2$ Bis(2,2′ -bipyridyl-4,4′-dicarbox-ylate)ruthenium(II) charge transfer sensitizers (x=C1⁻, Br⁻, I⁻, CN⁻, and SCN⁻) on nanocrystalline TiO$_2$ electrodes. J Am Chem Soc 1993; 115: 6382-90.

[7] Mathew S, Yella A, Gao P, Humphry-Baker R, CurchodBasile FE, Ashari-Astani N, Tavernelli I, Rothlisberger U, Nazeeruddin MK, Grätzel M. Dye-sensitized solar cells with 13% efficiency achieved through the molecular engineering of porphyrin sensitizers. Nat Chem 2014; 6: 242-7.

[8] Kakiage K, Aoyama Y, Yano T, Oya K, Fujisawa J-i, Hanaya M. Highly-efficient dye-sensitized solar cells with collaborative sensitization by silyl-anchor and carboxy-anchor dyes. Chem Commun 2015; 51: 15894-7.

[9] Vaghasiya JV, Sonigara KK, Soni SS, Tan SC. Dual functional hetero - anthracene based single component organic ionic conductors as redox mediator cum light harvester for solid state photoelectrochemical cells. J Mater Chem A 2018; 6: 4868-77.

[10] Vaghasiya JV, Sonigara KK, Suresh L, Panahandeh-Fard M, Soni SS, Tan SC. Efficient power generating devices utilizing low intensity indoor lights via nonradiative energy transfer mechanism from organic ionic redox couples. Nano Energy 2019; 60: 457-66.

[11] Liang M, Chen J. Arylamine organic dyes for dye-sensitized solar cells. Chem Soc Rev 2013; 42: 3453-88.

[12] Higashino T, Fujimori Y, Sugiura K, Tsuji Y, Ito S, Imahori H. Tropolone as a high- performance robust anchoring group for dye-sensitized solar cells. Angew Chem Int Ed 2015; 54: 9052-6.

[13] Liao XN, Zhang H, Huang JP, Wu GQ, Yin XL, Hong YP. (D-π-A) $_3$ -Type metal-free organic dye for dye-sensitized solar cells application. Dyes Pigments 2018; 158: 240-8.

[14] Kim BG, Chung K, Kim J. Molecular design principle of all-organic dyes for dye-sensitized solar cells. Chem Eur J 2013; 19: 5220-30.

[15] Bodedla GB, Justin Thomas KR, Fan M-S, Ho K-C. Benzimidazole-branched isomeric dyes: effect of molecular constitution on photophysical, electrochemical, and photovoltaic properties. J Org Chem 2016; 81: 640-53.

[16] Wenger S, Bouit P-A, Chen Q, Teuscher J, Censo DD, Humphry-Baker R, Moser J-E, Delgado JL, Martín N, Zakeeruddin SM, Grätzel M. Efficient Electron Transfer and Sensitizer Regeneration in Stable π-Extended Tetrathiafulvalene-Sensitized Solar Cells. J Am Chem Soc, 2010; 132: 5164-9.

[17] Patel DG, Bastianon NM, Tongwa P, Leger JM, Timofeeva TV, Bartholomew GP. Modification of nonlinear optical dyes for dye

sensitized solar cells: a new use for a familiar acceptor. J Mater Chem, 2011; 21: 4242-50.

[18] Zeng W, Cao Y, Bai Y, Wang Y, Shi Y, Zhang M, Wang F, Pan C, Wang P. Efficient dye-sensitized solar cells with an organic photosensitizer featuring orderly conjugated ethylenedioxythiophene and dithienosilole blocks. Chem Mater 2010; 22: 1915-25.

[19] Dai P, Yang L, Liang M, Dong H, Wang P, Zhang C, Sun Z, Xue S. Influence of the terminal electron donor in D-D-π-A organic dye sensitized solar cells: dithieno[3,2-b:2´,3´-d]pyrrole versus bis(amine). ACS Appl Mater Interfaces 2015; 7: 22436-47.

[20] Li WQ, Liu B, Wu YZ, Zhu SQ, Zhang Q, Zhu WH. Organic sensitizers incorporating 3,4-ethylenesioxythiophene as the conjugated bridge: Joint photophysical and electrochemical analysis of photovoltaic performance. Dyes Pigments, 2013; 99: 176-84.

[21] Seo KD, Choi IT, Park YG, Kang S, Lee JY, Kim HK, Novel D-π-A coumarin dyes containing low band-gap chromophores for dye-sensitised solar cells. Dyes Pigments, 2012; 94: 469-74.

[22] Xie Y, Wu W, Zhu H, LIU J, Zhang W, Tian H, Zhu W. Unprecedentedly targeted customization of molecular energy levels with auxiliary-group in organic solar cell sensitizers. Chem Sci. 2016: 7: 544-9.

[23] Zhang F, Luo TH, Song JS, Guo XZ, Liu WL, Ma CP, et al. Triphenylamine-based dyes for dye-sensitized solar cells. Dyes Pigment 2009; 81: 224-30.

[24] Jiang X, Karlsson KM, Gabrielsson E, Johansson EMJ, Quintana M, Karlsson M, Sun LC, Boschloo G, Hagfeldt A. Highly efficient solid-state dye-sensitized solar cells based on triphenylamine dyes. Adv Funct Mater 2011; 21: 2944-52.

[25] Tan LL, Huang JF, Shen Y, Xiao LM, Liu JM, Kuang DB, Sun CY. Highly efficient and stable organic sensitizers with duplex starburst triphenylamine and carbazole donors for liquid and quasi-solid-state dye-sensitized solar cells. J Mater Chem A 2014; 2: 8988-94.

[26] Song JS, Zhang F, Li CH, Liu WL, Li BS, Huang Y, Bo ZS. Phenylethyne-bridged dyes for dye-sensitized solar cells. J Phys Chem C 2009; 113: 13391-97.

[27] Cai LP, Tsao HN, Zhang W, Wang L, Xue ZS, Gr€atzel M, et al. Organic sensitizers with bridged triphenylamine donor units for efficient dye-sensitized solar cells. Adv Energy Mater 2013; 3: 200-5.

[28] Kima D, Kima C, Choia H, Songb K, Kangc MS, Koa J. A new class of organic sensitizers with fused planar triphenylamine for nanocrystalline dye sensitized solar cells. J Photochem Photobiol A 2011; 219: 122-31.

[29] Do K, Kim D, Cho N, Paek S, Song K, Ko J. New type of organic sensitizers with a planar amine unit for efficient dye-sensitized solar cells. Org Lett 2012; 14: 222-5.

[30] Zhao DX, Bian LY, Luo YX, Zhang MD, Cao H, Chen MD. Three-dimensional D-π-A organic sensitizer with coplanar triphenylamine moiety for dye-sensitized solar cells. Dyes Pigments 2017; 140: 278-85.

[31] Teng C, Yang, XC, Yang C, Li SF, Cheng M, Hagfeldt A, Sun LC. Molecular design of anthracene-bridged metal-free organic dyes for efficient dye-sensitized solar cells. J Phys Chem C 2010; 114: 9101–10.

[32] Teng C, Yang XC, Yang C, Tian HN, Li SF, Wang XN, Hagfeldt A, Sun LC. Influence of triple bonds as π-spacer Units in metal-free organic dyes for dye-sensitized solar cells. J Phys Chem C 2010; 114: 11305-13.

[33] Fang JK, Sun TX, Tian Y, Zhang YJ, Jin CF, Xu ZM, Fang Y, Hu XY, Wang HB. Novel diyne-bridged dyes for efficient dye-sensitized solar cells. Mate Chem Phys 2017; 195: 1-9.

[34] Fang JK, Hua XY, Xu MC, Wang HB, Zhang YJ, Jin CF, Zhong X. Molecular engineering of efficient organic sensitizers containing diyne-Bridge for dye-sensitized solar cells. Electrochimi Acta 2017; 253: 572-80.

[35] Torres É, Sequeira S, Parreira P, Mendes P, Silva T, Lobato K, Brites MJ. Coumarin dye with ethynyl group as p-spacer unit for dye sensitized solar cells. J Photoch Photobio A 2015; 310: 1-8.

[36] Singh P, Baheti A, Thomas KRJ, Lee CP, Ho KC. Fluorene-based organic dyes containing acetylene linkage for dye-sensitized solar cells. Dyes Pigments 2012; 95: 523-33.

[37] Chen YC, Chou HH, Tsai MC, Chen SY, Lin JT, Yao CF, Chen K. Thieno[3,4-b]thiophene-based organic dyes for dye-sensitized solar cells. Chem- Eur J 2012; 18: 5430 -37.

[38] Tian WW, Yi C, Song B, Qi Q, Jiang W, Zheng YP, Qi ZJ, Sun YM. Self-host homoleptic green iridium dendrimers based on diphenylamine dendrons for highly efficient single-layer PhOLEDs. J Mater Chem C, 2014; 2: 1104-15.

[39] Yuan R, Liu ZT, Wan Y, Liu Y, Wang YJ, Ge WH, Fang Y, Zhou SL, Han XE, Zhang P, Wu H. New D-D-π-A-type indol-triarylamine

sensitizers for efficient dye-sensitized solar cells. synthetic Met 2016; 215: 21-7.

[40] Wang HY, Chen G, Xu XP, Chen H, Ji SJ. The synthesis and photophysical properties of novel poly(diarylamino)styrenes. Dyes

Pigments, 2011: 88: 358-365.

[41] Vinayak MV, Lakshmykanth TM , Yoosuf M, Soman S, Gopidas K.R. Effect of recombination and binding properties on the

performance of dye sensitized solar cells based on propeller shaped triphenylamine dyes with multiple binding groups. Sol Energy 2016;

124: 227-41.

[42] Li QY, Wang ZC, Song WW, Ma HL, Dong JY, Quan YY, Ye XX, Huang ZS. A novel D-π-A triphenylamine-based turn-on

colorimetric and ratiometric fluorescence probe for cyanide detection. Dyes Pigments 2019; 161: 389-95.

[43] Gao WZ, Wang SR, Xiao Y, Li XG. Study on synthesis and properties of novel luminescent hole transporting materials based on N,

N´-di(p-tolyl)-N,N´ -diphenyl-1,1´-biphenyl-4,4 0 -diamine core. Dyes Pigments 2013; 97: 92-9.

[44] Lin J, Elangovan A, Ho T. Structure-property relationships in conjugated donor–acceptor molecules based on cyanoanthracene:

computational and experimental studies. J Org Chem 2005; 70: 7397-7407.

[45] Choi H, Lee JK, Son KH, Song K, Kang SO, Koa J. Synthesis of new julolidine dyes having bithiophene derivatives for solar cell.

Tetrahedron 2007; 63: 1553-1559.

[46] Zhang MD, Xie HX, Ju XH, Qin L, Yang QX, Zheng HG, Zhou XF. D-D-π-A organic dyes containing 4,4´-di(2-thienyl)-triphenyl-

Amine moiety for efficient dye-sensitized solar cells. Phys Chem Chem Phys 2013; 15: 634-41.

[47] Liang M, Xu W, Cai F, Chen P, Peng B, Chen J, Li Z. New triphenylamine-based organic dyes for efficient dye-sensitized solar cells

J Phys Chem C 2007; 111: 4465-72.

[48] Hara K, Dan-oh Y, Kasada C, Ohga Y, Shinpo A, Suga S, Sayama K, Arakawa H. Effect of additives on the photovoltaic performance

of coumarin-dye-sensitized nanocrystalline TiO_2 solar cells. Langmuir 2004; 20: 4205-4210.

[49] Hagfeldt A, Grätzel M. Light-induced redox reactions in nanocrystalline. Systems Chem. ReV. 1995; 95: 49-68.

[50] Li SL, Jiang KJ, Shao KF, Yang LM. Novel organic dyes for efficient dye-sensitized solar cells. Chem Commun 2006; 26: 2792-4.

[51] Wang HB, Bao BZ, Hu XY, Fang JK. Efficient small molecule organic dyes containing different bridges in donor moieties for dye-sensitized solar sells. Electrochimi Acta 2017; 250: 278-84.

[52] Fernandes SSM, Mesquita I, Andrade L, Mendes A, Justino L LG, Burrows HD, Raposo MMM. Synthesis and characterization of push-pull bithiophene and thieno [3, 2-b]thiophene derivatives bearing an ethyne linker as sensitizers for dye-sensitized solar cells. Org Electron 2017; 49: 194-205.

[53] Elmorsy, MR, Su R, Fadda AA., Etman HA, Tawfik EH, El-Shafei A. Molecular engineering and synthesis of novel metal-free organic sensitizers with D-π-A-π-A architecture for DSSC applications: The effect of the anchoring group. Dyes Pigments 2018; 158: 121-30.

[54] Xie YS, Wu WJ, Zhu HB, Liu JC, Zhang WW, Tian H, Zhu WH. Unprecedentedly targeted customization of molecular energy levels with auxiliary-group in organic solar cell sensitizers. Chem Sci 2016; 7: 544-9.

[55] Ma XM, Wu WJ, Zhang Q, Guo FL, Meng FS, Hua JL. Novel fluoranthene dyes for efficient dye-sensitized solar cells. Dyes Pigments 2009; 82: 353-9.

[56] Xiang HD, Fan Wei, Li JH, Li TY, Robertson Neil, Song XR, Wu WJ, Wang ZH, Zhu WH, Tian H. High-performance porphyrin-based dye-sensitized solar cells with iodine and cobalt redox shuttles. Chem Sus Chem 2017; 10: 938- 45.

[57] Mathew S, Yella A, Gao P, Humphry-Baker R, Curchod BF, Ashari-Astani N, Tavernelli I, Rothlisberger U, Nazeeruddin MK, Grätzel M. Dye-sensitized solar cells with 13% efficiency achieved through the molecular engineering of porphyrin sensitizers. Nat Chem 2014; 6: 242-247.

[58] Liu JC, Liu B, Tang YY, Zhang WW, Wu WJ, Xie YS, Zhu WH. Highly efficient cosensitization of D-A-π–A benzotriazole organic dyes with porphyrin for panchromatic dye-sensitized solar cells. J Mater Chem C, 2015; 3: 11144-150.

Highlights

Two novel dyes designed with a 4-methoxyphenyl group.

4-methoxyphenyl & ethynyl group with an axial-symmetric conjugated system significantly

promote the intramolecular charge transfer process.

The power conversion efficiency of 6.37% reaching from 3.43% under optimum condition.

Declaration of interests

☒ The authors declare that they have no known competing financial interests or personal relationships that could have appeared to influence the work reported in this paper.

☒The authors declare the following financial interests/personal relationships which may be considered as potential competing interests:

The authors declare that they have no known competing financial interests or personal relationships .